International Journal of Minerals, Metallurgy and Materials
Volume 21, Number 8, August 2014, Page 772
DOI: 10.1007/s12613-014-0970-1

Arc characteristics of submerged arc welding with stainless steel wire

Ke Li, Zhi-sheng Wu, Cui-rong Liu, and Feng-hua Chen

College of Materials Science and Engineering, Taiyuan University of Science and Technology, Taiyuan 030024, China
(Received: 17 December 2013; revised: 16 March 2014; accepted: 19 March 2014)

Abstract: The arc characteristics of submerged arc welding (SAW) with stainless steel wire were studied by using Analysator Hannover (AH). The tests were carried out under the same preset arc voltage combined with different welding currents. By comparing the probability density distribution (PDD) curves of arc voltage and welding current, the changes were analyzed, the metal transfer mode in SAW was deduced, and the characteristics of a stable arc were summarized. The analysis results show that, with an increase of welding parameters, the short-circuiting peak in the PDD curves of arc voltage decreases gradually until it disappears, and the dominant metal transfer mode changes from flux-wall guided transfer to projected transfer and then to streaming transfer. Moreover, when the PDD curves of arc voltage are both unimodal and generally symmetrical, the greater the peak probability and the smaller the peak span, the more stable the arc becomes.

Keywords: submerged arc welding; electric arc; characteristics; stainless steel; wire; metal transfer

1. Introduction

To save precious metal and lower production costs, some mechanical components, such as rollers and plungers, are designed by making a stainless steel weld overlay on a mild steel substrate to obtain a special anticorrosive and wear-resisting surface [1−3]. In the manufacturing industry, submerged arc welding (SAW) has been widely applied due to its low pollution level, high efficiency, good quality welds, and high degree of automation [4]. Experience shows that the arc stability directly affects the properties of the surfacing layer [5], so studies on the arc characteristics, especially the arc stability, have important significance for improving the surfacing layer's quality and welding process automation.

With the help of high-speed video cameras and oscilloscopes, many previous researchers have studied the arc shape and metal transfer in manual electrode welding and gas-shielded arc welding. Wang *et al.* [6] pointed out that there are four basic metal transfer modes, including globular, explosive, spray, and flux-wall guided transfer for covered electrodes. With the assistance of statistical data collected by Analysator Hannover (AH), they accurately described the arc physical characteristics for different metal transfer modes and proposed a quantitative method to determine the metal transfer mode for different covered electrodes. Rhee and Kannatey-Asibu [7] observed different metal transfer modes in gas metal arc welding using a digital high-speed video analyzer and an arc shadow-graphing system. Kim and Eagar [8–9] used a static force balance theory to estimate the melting rates of the electrodes during pulsed gas metal arc welding. The model was found to be in good agreement with experimental results when the base current and the load duty cycle were small. Li *et al.* [10] studied the metal transfer of gas-shielded flux-cored wire by high-speed photographic experiments with a He-Ne laser as a back-ground light source. The observed results showed that an incompletely melting slag column existed between the end of the electrode and the welding pool, which was favorable for stabilizing metal transfer and decreasing spatter, but, even so, short-circuiting transfer progressed smoothly. Ghosh *et al.* [11] investigated the arc characteristics and behavior of metal transfer in pulsed current gas metal arc welding with austenitic stainless steel filler wire by high-speed video photography. It was found that an increase of factor ϕ related to welding parameters from 0.05 to 0.27 enhanced the arc length, root and projected diameter of arc

Corresponding author: Zhi-sheng Wu E-mail: wuzstyust@163.com

and droplet diameter, whereas it reduced the arc pressure and droplet velocity.

Studies on SAW arc characteristics are, however, very rarely reported. The reason may be that the arc of SAW buried under flux layers are invisible, so it is difficult to observe the arc shape and the metal transfer using traditional visual sensing technologies. In this study, AH was used to detect the electric signals of SAW with stainless steel wire. Based on a comprehensive analysis of statistical data and curves, an evaluation approach for welding arc stability was proposed. The metal transfer modes in SAW were also deduced, which provides a basis for establishing reasonable welding parameters and achieving welding process automation.

AH is a high speed data acquiring and processing system, which can sample electrical signals of voltage and current in real time at a speed of 2×10^5 points per second. It can also statistically analyze data using its own software [12–13]. In short, the AH test is nowadays the latest technique for measuring welding electric parameters.

2. Experimental

The arc characteristics were studied by flat depositing on a mild steel plate. The welding machine was MZ–1250 and the SAW process was operated under direct current electrode positive (DCEP). Three stainless steel wires were selected to form the weld beads, which included two solid wires and one flux-cored wire. Welding materials and parameters used in the tests are listed in Table 1. During the welding process, the electrical signals were recorded by AH in real time within 5 s. The connection diagram of the experimental apparatus is shown in Fig. 1.

Table 1. Materials and parameters used in the tests

Electrode (AWS)	Wire type	Electrode diameter / mm	Preset voltage / V	Welding current / A	Welding speed / (mm·min^{-1})	Electrode extension / mm	Plate thickness / mm	Flux
ER420	Solid	3.2	40	400–600	350	40	10	HJ260
ER410NiMo	Flux-cored	3.2	40	330–530	350	35	10	HJ260
ER420J	Solid	4.0	40	550–790	350	45	20	HJ260

Note: AWS — American Welding Society.

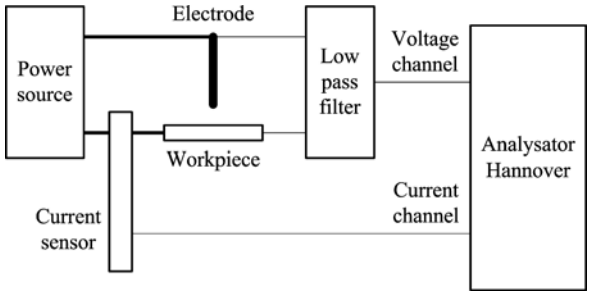

Fig. 1. Connection diagram of experimental apparatus.

3. Results and discussion

According to the actual mean value of the welding current, all test data were distributed to three regions (lower, medium, and higher). Each region contained six groups of test data. The characteristic values of the three wires obtained by AH are listed in Tables 2–4.

3.1. Characteristics under lower welding parameters

Fig. 2 shows the PDD curves of arc voltage and welding current under lower welding parameters for ER420. As can be seen from Fig. 2(a), the three curves all have a lower peak and a higher peak. The left lower peak in the low voltage range is the short-circuiting peak, which reflects short-circuiting features. The right higher peak in the welding voltage range is the arcing peak, it attributes to arc burning characteristics. Further analysis indicates that, at a lower welding current, the molten droplet can grow to a large size before detachment because the electromagnetic pinch force promoting droplet detachment from the electrode tip is weak. This results in globular transfer. Meanwhile, low voltage indicates that the arc length is short. The result is that, when large droplets fall down through a short arc, short-circuiting easily occurs between the bottom of the molten droplet and the surface of the weld pool. However, in SAW, owing to the existence of surface tension and the molten slag, parts of droplets may be attracted or repelled to the inner wall of the molten flux layer and flow along with it. This is called flux-wall guided transfer [14]. The probability of short-circuiting is consequently very small (< 0.1%). Moreover, with an increase in welding current, the droplet size becomes smaller and the arc length becomes longer, so the probability of short-circuiting decreases and that of stable arcing increases gradually, corresponding to the display in Fig. 2(a), where the short-circuiting peak decreases and the arcing peak increases in turn. In addition, at the far right of the curves, some jagged curves appear at the high voltage

range with their maxima near 100 V. This is caused by arc jumping from the droplet bottom to the pinch neck after the detachment of a large droplet. Fig. 2(b) shows the PDD curves of welding current for three groups of lower welding parameters. These show that the positions of three peaks shift to the right in turn and the peak values increase gradually, indicating that the arc stability improves with an increase in welding current.

Table 2. Test data of ER420 obtained by AH

Welding parameter region	Welding current				Arc voltage			
	Mean / A	Peak probability / %	Current of peak probability / A	Peak span (> 0.1%) / A	Mean / V	Peak probability / %	Voltage of peak probability / V	Peak span (> 0.1%) / V
Lower	416.09	1.0876	468.750	314.69	28.99	3.8632	30.625	16.50
	422.00	1.0440	470.703	318.36	28.00	4.3762	30.125	15.00
	431.85	1.2008	494.141	279.30	30.13	4.4242	31.000	15.25
	453.52	1.3818	498.047	244.14	32.55	5.0690	33.000	14.00
	467.55	1.4492	500.000	240.23	32.69	5.0852	33.125	13.25
	477.23	1.4782	511.719	251.95	33.50	5.2474	35.000	13.75
Medium	485.78	1.4618	519.531	253.91	34.13	5.3578	35.250	12.75
	493.23	1.4596	525.391	248.05	35.39	5.5698	35.500	11.75
	505.52	1.5796	535.156	248.05	36.12	5.6976	36.000	12.00
	518.69	1.5434	519.531	249.30	36.66	5.5548	36.500	12.25
	529.42	1.6284	542.969	246.09	38.21	5.3544	37.500	12.00
	535.75	1.5942	562.500	265.63	37.04	5.0492	36.750	12.25
Higher	543.45	1.5384	562.500	269.53	38.82	4.9516	38.250	13.00
	550.37	1.4942	552.734	281.49	39.85	4.4898	39.250	13.50
	562.73	1.3474	537.109	308.59	40.49	4.3964	40.000	14.00
	573.80	1.1954	542.969	375.47	45.29	3.3958	45.250	15.00
	585.93	0.9652	517.726	451.62	45.95	3.2420	45.250	16.00
	590.97	0.9332	514.453	475.24	45.09	3.1442	43.250	17.75

Table 3. Test data of ER410NiMo obtained by AH

Welding parameter region	Welding current				Arc voltage			
	Mean / A	Peak probability / %	Current of peak probability / A	Peak span (> 0.1%) / A	Mean / V	Peak probability / %	Voltage of peak probability / V	Peak span (> 0.1%) / V
Lower	341.06	0.9660	421.875	289.52	24.74	3.2148	23.000	17.25
	345.59	1.0342	414.063	285.39	24.43	3.2306	24.125	16.50
	360.54	1.0838	439.453	280.99	25.69	3.3428	25.500	16.00
	374.98	1.1730	439.453	276.50	28.46	3.4966	27.250	17.00
	382.94	1.2438	439.453	274.59	26.94	2.5182	28.250	15.75
	397.84	1.2578	462.891	270.16	29.11	4.0648	29.500	15.50
Medium	403.03	1.2746	453.125	267.88	28.20	4.7028	31.000	14.50
	415.65	1.2448	470.703	263.39	30.95	4.6462	31.750	15.25
	421.00	1.2792	470.703	261.48	29.87	6.5398	30.750	15.75
	429.23	1.4658	478.516	259.77	31.43	5.9584	33.500	13.75
	440.63	1.3972	490.234	265.63	32.31	5.0754	34.125	14.25
	446.77	1.2444	498.047	275.39	33.50	4.3576	34.500	14.00
Higher	461.11	1.3096	498.047	277.34	34.94	3.6422	35.500	13.50
	473.70	1.3020	494.141	281.25	37.77	4.1278	37.750	15.00
	481.96	1.2864	503.438	283.20	36.14	4.0052	36.000	14.00
	489.43	1.2332	509.531	292.97	40.55	3.6412	40.250	14.50
	493.89	1.2340	519.531	321.26	39.60	3.7948	40.000	14.75
	515.73	1.2210	513.672	328.12	43.78	3.3566	42.750	17.25

Table 4. Test data of ER420J obtained by AH

Welding parameter region	Welding current				Arc voltage			
	Mean / A	Peak probability / %	Current of peak probability / A	Peak span (> 0.1%) / A	Mean / V	Peak probability / %	Voltage of peak probability / V	Peak span (> 0.1%) / V
Lower	552.45	0.8463	564.953	414.06	33.75	3.1940	35.500	13.25
	558.29	1.0187	553.234	429.69	34.15	4.1190	37.000	14.00
	574.66	1.0654	564.953	392.58	34.70	4.7177	36.250	12.25
	580.98	1.0707	572.766	398.44	36.01	5.0023	37.000	11.75
	594.59	1.1108	566.906	386.72	35.36	5.1893	35.750	11.25
	610.66	1.1330	568.859	365.23	37.29	5.5328	37.500	11.75
Medium	622.59	1.1117	584.484	365.23	37.84	5.8382	37.750	11.00
	645.83	1.1517	590.344	356.33	39.53	5.8662	39.000	10.50
	657.19	1.1718	594.250	355.47	39.08	5.9856	38.500	10.25
	671.36	1.2587	609.434	332.27	40.26	6.2078	39.750	10.00
	685.66	1.1568	627.453	341.80	40.45	5.8460	39.500	10.25
	698.51	1.0133	602.063	341.80	41.82	5.7330	40.750	10.25
Higher	714.43	0.9173	627.453	357.42	41.79	5.5923	41.500	11.00
	724.79	0.9483	627.453	363.28	42.30	5.3967	41.500	11.25
	740.54	0.8730	629.406	375.00	42.99	4.7313	42.250	11.00
	751.44	0.8243	654.797	390.63	42.54	4.7833	41.250	11.25
	770.90	0.8413	660.656	402.34	43.73	4.7530	43.000	12.25
	782.29	0.7710	689.953	404.30	44.92	4.3533	44.250	14.00

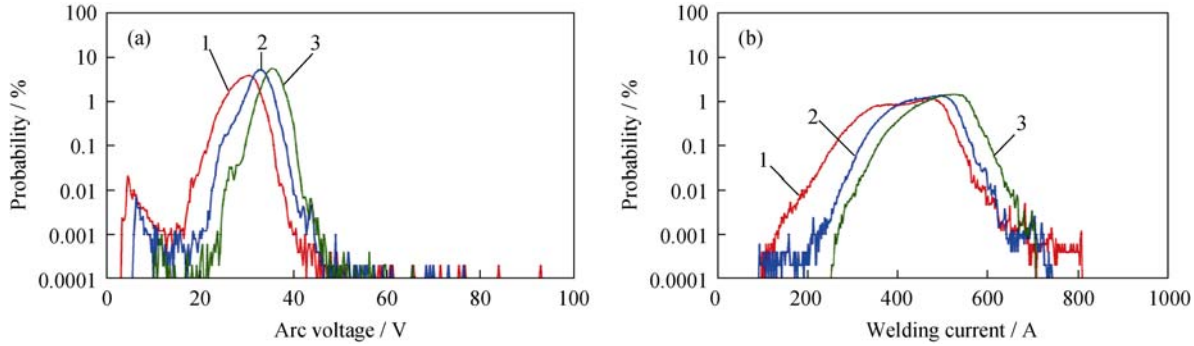

Fig. 2. PDD curves of (a) arc voltage and (b) welding current under lower welding parameters for ER420 (1—28.00 V and 422.00 A; 2—32.55 V and 453.52 A; 3—33.50 V and 477.23 A).

3.2. Characteristics under medium welding parameters

Fig. 3 shows the PDD curves of arc voltage and welding current under medium welding parameters for ER420. It can be seen from Fig. 3(a) that, with an increase of welding parameters, the short-circuiting peak continues to decline until it disappears at 505.52 A. Meanwhile, the arcing peaks of the three curves have almost the same peak probability and peak span, but they are higher and narrower than those of the lower parameters. The reason may be that most fine droplets transit in projected transfer mode at higher welding current. Of course, there are still some droplets undergoing flux-wall guided transfer, and there are a few short-circuiting transfers. Under these conditions, the metal transfer is relatively stable over a wide range of voltage because of the moderate arc length, good arc stiffness, and smaller droplet size. Additionally, as the droplets become smaller, the voltage of the sawtooth curves at the far right caused by arc jumping, reduces to less than 80 V. Fig. 3(b) shows that the three curves do not differ much in peak or span, but the peak span is significantly reduced compared to that of the lower parameters.

3.3. Characteristics under higher welding parameters

Fig. 4 shows the PDD curves of arc voltage and welding current under higher welding parameters for ER420. Fig. 4(a)

shows that all curves only have an arcing peak and reveal a similar shape except for the position and height. The reason may be that, with further increase in the welding parameters, the extremely large electromagnetic pinch force causes the droplet size to reduce further and the transfer rate to increase rapidly. In this case, a large number of fine droplets are propelled across the long arc towards the weld pool, streaming transfer becomes the dominant transfer mode, and only a small number of droplets experience flux-wall guided transfer by colliding with the inner wall of the molten flux slag, so there is absolutely no short-circuiting transfer. In addition, the peak spans of three curves increase in turn. Fig. 4(b) shows that the peaks of three curves decrease in turn. There is little difference in the low current range, but the probability increases in the current range above 700 A and the peak span increases in turn.

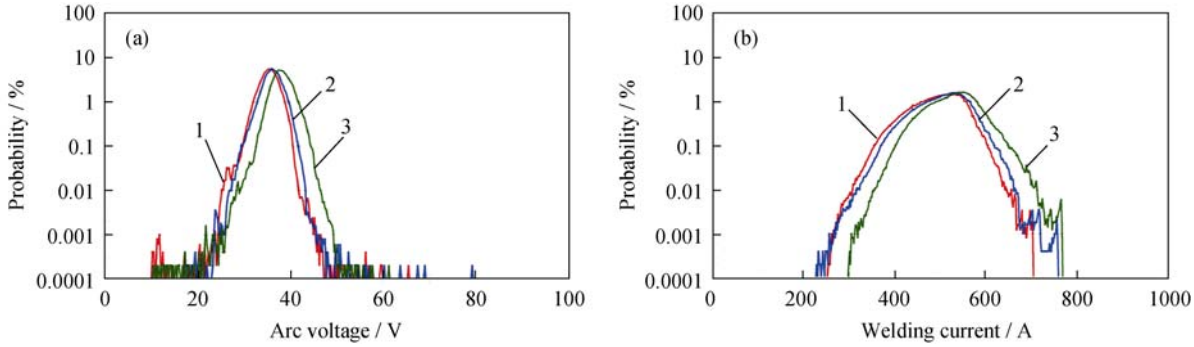

Fig. 3. PDD curves of (a) arc voltage and (b) welding current under medium welding parameters for ER420 (1—35.39 V and 493.23 A; 2—36.12 V and 505.52 A; 3—38.21 V and 529.42 A).

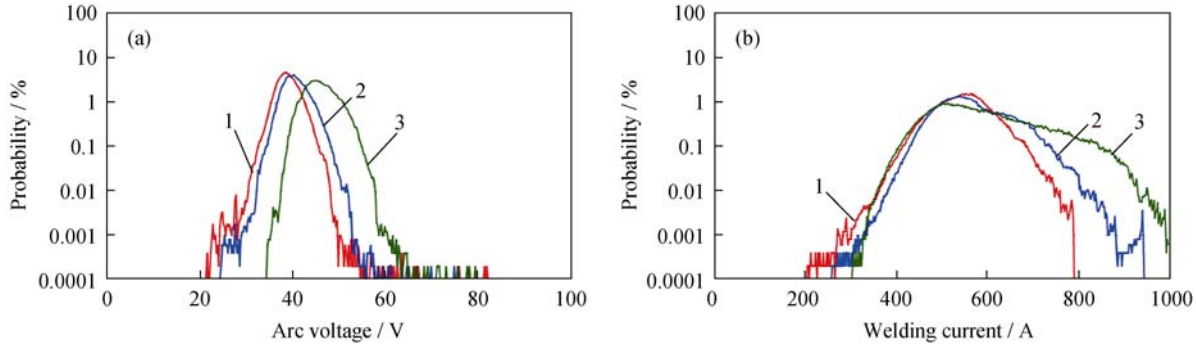

Fig. 4. PDD curves of (a) arc voltage and (b) welding current under higher welding parameters for ER420 (1—38.82 V and 543.45 A; 2—40.49 V and 562.73 A; 3—45.95 V and 585.93 A).

3.4. Comparison of three different welding parameter regions

The PDD curves of arc voltage and welding current under different welding parameter regions for the three wires are compared in Figs. 5–7. Overall, the three types of wires have much in common. From the voltage PDD curves, it can be seen that two peaks exist for the lower welding parameters, while under medium parameters, the short-circuiting peak disappears, the arcing peak is the highest, and the peak span is the narrowest. When under the higher parameters, the arcing peak declines, and the peak span widens. Further observation shows that, for the medium parameters, the gradient before and after the arcing peak is approximately symmetrical, but those of the other two categories are not so. For the lower parameters, the front is slow, and the back is steep; for the higher parameters, the front is steep, and the back is slow. This is caused by different arc stiffnesses in different voltage ranges. Obviously, the arc has the best stiffness under the medium parameters. In other words, the PDD curves for the medium parameters are the most concentrated of the three regions, which indicates that the arc stability under these conditions is the best. On the other hand, the current PDD curves reveal large differences in peak span: ER420J is the widest, ER410NiMo is the narrowest, and ER420 is between them. The main reason is the different heat inputs that each requires: for the same diameter, flux-cored wire needs a less heat input than solid wire, while for two solid wires of different diameters, the larger diameter wire needs a greater heat input.

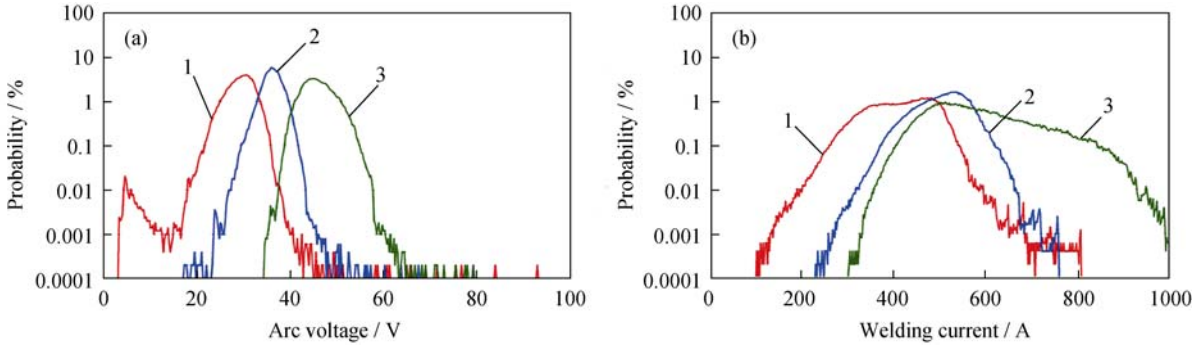

Fig. 5. PDD curves of (a) arc voltage and (b) welding current under different welding parameter regions for ER420 (1—28.00 V and 422.00 A; 2—36.12 V and 505.52 A; 3—45.95 V and 585.93 A).

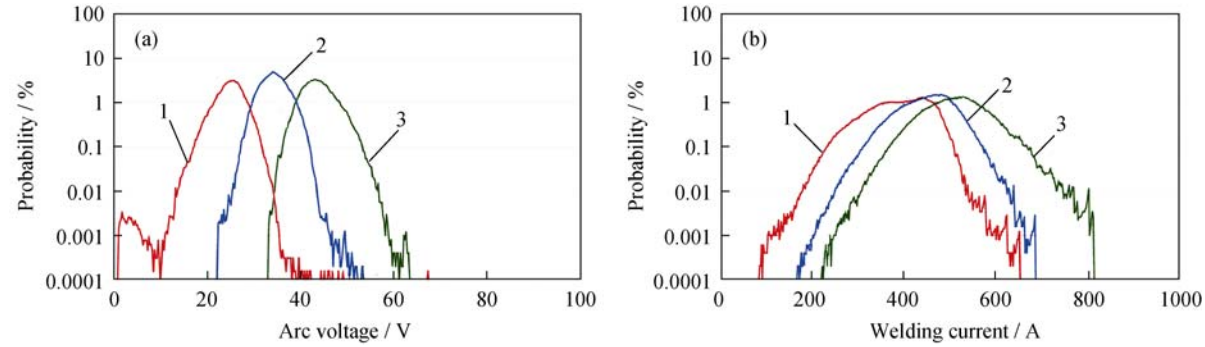

Fig. 6. PDD curves of (a) arc voltage and (b) welding current under different welding parameter regions for ER410NiMo (1—24.43 V and 345.59 A; 2—31.43 V and 429.23 A; 3—43.78 V and 515.73 A).

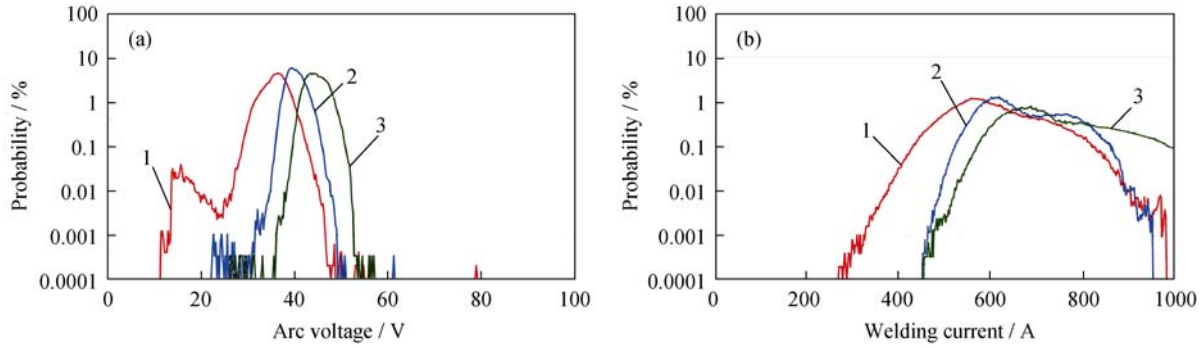

Fig. 7. PDD curves of (a) arc voltage and (b) welding current under different welding parameter regions for ER420J (1—35.36 V and 594.59 A; 2—40.26 V and 671.36 A; 3—44.92 V and 782.29 A).

All of the above analyses show that, in SAW, when the PDD curves of arc voltage are unimodal and generally symmetrical, the greater the peak probability and the smaller the peak span, the better is the arc stability.

4. Conclusions

Arc characteristics of SAW with stainless steel wire under different welding parameters were studied by AH, and the metal transfer modes in SAW were deduced. The following conclusions are drawn.

(1) With an increase of welding parameters in SAW, the short-circuiting peak in the PDD curve of arc voltage decreases gradually until it disappears, while the arcing peak increases first and then decreases. The peak span first decreases and then increases. The PDD curve of welding current has only one peak, and the change of the peak is similar to that of the arc voltage peak.

(2) A changing metal transfer mode is the primary cause of variation in the PDD curves for the electric signals. With increasing welding parameters, the droplet size gradually becomes smaller and smaller. At lower welding parameters, the dominant metal transfer mode is flux-wall guided transfer. This changes to projected transfer mode under medium

parameters, and streaming transfer plays the main role under higher parameters.

(3) In SAW, when the PDD curves of arc voltage are both unimodal and generally symmetrical, the greater the peak probability and the smaller the peak span, the better the arc stability is.

Acknowledgements

This work was financially supported by the Shanxi Provincial Key Programs for Science and Technology Development (No. 20100321084) and Taiyuan Special Foundation for Excellent Talents (No. 20111075).

References

[1] B.X. Hu, K.L. Mang, J.G. Wang, and B.S. Xu, Application of surfacing on mechanism equipments maintaining of petroleum chemical industry and metallurgy industry in China, *China Surf. Eng.*, 19(2006), No. 3, p. 4.

[2] Y.Y. Zhang, Y.F. Bao, Y.F. Jiang, and K. Yang, Present status and development trend of roll surfacing technology, *Electr. Weld. Mach.*, 40(2010), No. 10, p. 17.

[3] D. Govardhan, A.C.S. Kumar, K.G.K. Murti, and G. Madhusudhan Reddy, Characterization of austenitic stainless steel friction surfaced deposit over low carbon steel, *Mater. Des.*, 36(2012), p. 206.

[4] A. Singh, S. Datta, S.S. Mahapatra, T. Singha, and G. Majumdar, Optimization of bead geometry of submerged arc weld using fuzzy based desirability function approach, *J. Intell. Manuf.*, 24(2013), No. 1, p. 35.

[5] J. Wang, M.X. Lu, L. Zhang, W. Chang, L.N. Xu, and L.H. Hu, Effect of welding process on the microstructure and properties of dissimilar weld joints between low alloy steel and duplex stainless steel, *Int. J. Miner. Metall. Mater.*, 19(2012), No. 6, p. 518.

[6] B. Wang, L. Yang, and Y. Wang, Evaluation of typical metal transfer modes for covered electrode, *Trans. China Weld. Inst.*, 27(2006), No. 11, p. 95.

[7] S. Rhee and E. Kannatey-Asibu Jr, Observation of metal transfer during gas metal arc welding, *Weld. J.*, 71(1992), No. 10, p. 381-s.

[8] Y.S. Kim and T. W. Eagar, Metal transfer in pulsed current gas metal arc welding, *Weld. J.*, 72(1993), No. 7, p. 279-s.

[9] Y.S. Kim and T.W. Eagar, Analysis of metal transfer in gas metal arc welding, *Weld. J.*, 72(1993), No. 6, p. 269-s.

[10] H. Li, W.S. Cao, B.G. Chen, and X.B. Sun, Metal transfer of gas shielded flux cored wire and its characteristics, *Trans. China Weld. Inst.*, 21(2000), No. 1, p. 13.

[11] P.K. Ghosh, L. Dorn, S. Kulkarni, and F. Hofmann, Arc characteristics and behaviour of metal transfer in pulsed current GMA welding of stainless steel, *J. Mater. Process. Technol.*, 209(2009), p. 1262.

[12] C.S. Wu, T. Polte, and D. Rehfeldt, A fuzzy logic system for process monitoring and quality evaluation in GMAW, *Weld. J.*, 80(2001), No. 2, p. 33.

[13] B. Wang, Y.L. Song, and D. Rehfeldt, Analysis and evaluation of the usability of welding consumables, *Electr. Weld. Mach.*, 36(2006), No. 11, p. 11.

[14] D.W. Cho, W.H. Song, M.H. Cho, and S.J. Na, Analysis of submerged arc welding process by three-dimensional computational fluid dynamics simulations, *J. Mater. Process. Technol.*, 213(2013), No. 12, p. 2278.